

Interacting associations between ploidy, breeding system, and lineage diversification

Rosana Zenil-Ferguson,¹ J. Gordon Burleigh,² William A. Freyman,³ Boris Igić,⁴ Itay Mayrose,⁵ and Emma E. Goldberg⁶

¹University of Minnesota Twin Cities

²University of Florida

³23 and me

⁴University of Illinois

⁵Tel Aviv University

⁶University of Minnesota Twin Cities

Author for correspondence: Rosana Zenil-Ferguson

Running head: Ploidy and breeding systems in Solanaceae

Keywords: Polyploidy, Breeding System, Diversification, SSE models

Abstract

The effect of polyploidy in diversification remains a contentious issue. On the one hand, recent studies that found that polyploids have slower speciation rates and higher extinction rates than diploids left scientist wondering if polyploidy is truly an evolutionary dead-end. On the other hand, botanist have found strong
5 molecular support of multiple polyploidy events at the root of highly diverse clades which challenges the evolutionary dead-end conclusions reached by modeling approaches. We re-investigate the role of polyploidy in speciation and extinction from a new modeling perspective considering that patterns found in diversification models can be misleading and incorrectly attributed to polyploidy when other observed and unobserved plant traits are responsible of shaping diversification. Using statistically robust comparative
10 phylogenetic approaches, we show that it is possible to detect whether the contribution of polyploidy to speciation and extinction is significant under the presence of other potential traits also affect diversification. We use the phylogeny, polyploidy, and breeding system data of 595 Solanaceae species to understand the contribution of polyploidy to diversification. We ask if Solanaceae polyploids are evolutionary dead-ends, and whether breeding system or some other unobserved traits are responsible of the patterns of diversification
15 observed in the phylogeny.

Introduction

The systematic search for traits which influence the rates at which species accumulate around the tree of life is at the productive confluence of drastic increases in the size of datasets and equally dramatic improvements in analytical methods (Maddison et al. 2007; FitzJohn et al. 2009; Goldberg and Igić 2012; Beaulieu and O'Meara 2016). Many limitations impede our progress in identifying estimating trait-dependent differences in speciation and extinction rates (Maddison and FitzJohn 2014; Rabosky and Goldberg 2015). Nevertheless, the field has made steady advances in relaxing assumptions and addressing conceptual difficulties. One limitation is the pervasive consideration of traits in isolation. For example, studies commonly aim to identify the effects of alternate states of a single trait on the diversification process. This is problematic, because the context in which traits occur can lead to complex interactions, perhaps with other traits that make up an organism or its environment. Consequently, an obvious direction for improvement of trait-dependent diversification models ought to involve development of approaches that allow investigation of individual and joint effects of traits on diversification, as well as each other's state transitions. Ideally, the initial application of such approaches ought to rely on well-sampled and studied traits, whose interactions are relatively clear, and which show a wide phylogenetic distribution. In this paper, we use two of the best studied traits in flowering plants, ploidy and breeding system, and demonstrate an approach to consider their individual and joint effects on diversification.

The prevalence of variation in chromosome number, and especially ploidy, has been broadly considered a salient feature of flowering plants for nearly a century. The recent dramatic increase in the scale of available genome sequences uncovered ancient rounds of whole-genome duplications, and subsequent re-diploidization, across angiosperms (Lynch and Conery 2000; Vision et al. 2000). Nearly all lineages of flowering plants are thought to have undergone at least one or two rounds of polyploidization. It is therefore surprising that there is little agreement regarding the evolutionary consequences of polyploidy, especially how it affects diversification rates.

Polyploidization alters the genomic content of all cells, and consequently has the potential to affect a wide variety, if not all, traits. From the very beginning, the study of this cytogenetic property considered correlations with other traits (Stebbins 1938). Among the many of changes associated with polyploidization, perhaps the most prominent is the association between polyploidy and propensity for self-fertilization (Stebbins 1950; Barrett 1988). Polyploidy is not only a suspected correlate of breeding systems but a causal link (Stout and Chandler 1942; Lewis 1947). Doubled number of alleles in pollen is strongly suspected to effect disruption of the genetic mechanisms in gametophytic self-incompatibility systems (Entani et al.

1999; Tsukamoto et al. 2005; Kubo et al. 2010). Polyploidy is also thought to be associated with changes in the rate of self-fertilization, although the evidence for this correlated shift in mating system appears limited and sometimes contradictory (Barringer 2007; Barrett 2008; Husband et al. 2008).

Breeding system shifts—changes in the collection of physiological and morphological traits that determine the likelihood that any two gametes unite—are remarkably common and affect the distribution and amount of genetic variation in populations (Stebbins 1974; Barrett 2013). They are by themselves thought to have a broad effect on other traits. The frequent transition from self-incompatibility (SI) to self-compatibility (SC) is strongly associated with net diversification rate changes (Goldberg et al. 2010; de Vos et al. 2014). Given that changes in ploidy and breeding systems may be causally related and have profound effects on the fate of lineages, it seems particularly profitable to examine whether and how their macroevolutionary effects interact. Moreover, increases in ploidy are known to directly affect breeding system states and present a rare opportunity for the study of paths and path-dependence on trait evolution and diversification. For example, we could ask if the ordinary mutation (and fixation) causes more losses of SI than polyploidization, whether more SC polyploids are generated directly, after polyploidization of diploid SI lineages, or through a two-step pathway, involving loss of SI and subsequent polyploidization of a SC lineage. And, are diversification rates of polyploid SC lineages different if one or other path was taken? Charlesworth (1985)

Here, we [...]

Methods

Data

Chromosome number data were obtained for all Solanaceae taxa in the Chromosome Counts Database (CCDB; Rice et al. 2015), and the ca. 14,000 records were cleaned semi-automatically using the CCDBcurator R package (Rivero et al. 2019). This large dataset includes the compilation of Solanaceae ploidy states from Robertson et al. (2011). Species were coded as either diploid (D) or polyploid (P). For the majority of species, ploidy was assigned according to information from the original publications and the Kew Royal Botanic Gardens C-value DNA resource (Bennett and Leitch 2005). For taxa without ploidy information but with information about chromosome number, we assigned ploidy based on the multiplicity of chromosomes within the genus. For example, *Solanum betaceum* did not include information about ploidy level but it has 24 chromosomes, so because $x = 12$ is the base chromosome number of the *Solanum* genus (Olmstead and Bohs 2007), we assigned *S. betaceum* as diploid. Species with more than one ploidy level were assigned the smallest and most frequent ploidy level recorded. Breeding system was scored as self-incompatible (I) or

self-compatible (C) based on results curated from the literature and original experimental crosses (as compiled in Igić et al. 2006; Goldberg et al. 2010; Robertson et al. 2011; Goldberg and Igić 2012). Most species
80 could unambiguously be coded as either I or C (Raduski et al. 2012). Following previous work, we coded as I any species with functional I systems, even if C or dioecy was also reported. Dioecious species without functional I were coded as C.

To those existing data sets, we added some additional records for chromosome number and breeding system. The Supplementary Information contains citations for the numerous sources for the added data.
85 Resolution of taxonomic synonymy followed the conventions provided in Solanaceae Source (PBI *Solanum* Project 2012). Hybrids and cultivars were excluded because ploidy and breeding system can be affected by artificial selection during domestication. Following the reasoning outlined in Robertson et al. (2011), we examined closely the few species for which the merged ploidy and breeding system data indicated the presence of self-incompatible polyploids. Although SI populations frequently contain some SC individuals,
90 and diploid populations frequently contain some polyploid individuals, in no case did we find a convincing case of a naturally occurring SI and polyploid population. The single instance of an SI and polyploid individual appears to be an allopolyploid hybrid of *Solanum oplocense* Hawkes x *Solanum gourlayii* Hawkes, reported by Camadro and Peloquin 1981. Under exceedingly rare circumstances, it is possible for polyploids containing multiple copies of S-loci to remain SI, so long as they express a single allele at the S-locus
95 (discussed in Robertson et al. 2011). Because of the resulting absence of SI and polyploid populations, as well as the linked functional explanation for disabling of gametophytic self-incompatibility systems with non-self recognition, following whole genome duplication (reviewed in Ramsey and Schemske 1998; Stone 2002), we consider only three observed character states: self-incompatible diploids (ID), self-compatible diploids (CD), and polyploids which are always self-compatible (CP).

100 Matching our character state data to the largest time-calibrated phylogeny of Solanaceae (Särkinen et al. 2013) yielded 595 species with ploidy and/or breeding system information on the tree. Binary or three-state classification of ploidy and breeding system for the 595 taxa is summarized in Fig. 1. We retained all of these species in each of the analyses below because pruning away tips lacking breeding system in the ploidy-only analyses (and vice versa) would discard data that could inform the diversification models. A total of 405
105 taxa without any information about breeding system or polyploidy were excluded. Tips without trait data are much less informative for diversification parameters linked to trait values. Including this many more species would have prohibitively slowed our analyses, especially those implementing the most complex models.

Models for ploidy and diversification

To investigate the association between ploidy level and diversification, we first defined a binary state speciation and extinction model (BiSSE, Maddison et al. 2007) in which taxa were classified as diploid (D) or polyploid (P) (Fig. 1). We call this the *D/P ploidy* model. In a Bayesian framework, we obtained posterior probability distributions of speciation rates (λ_D, λ_P), extinction rates (μ_D, μ_P), net diversification rates ($r_D = \lambda_D - \mu_D, r_P = \lambda_P - \mu_P$), and relative extinction rates ($v_D = \mu_D/\lambda_D, v_P = \mu_P/\lambda_P$) associated with each state. This analysis explores the same question as Mayrose et al. (2011, 2015), but our analyses differ because we include not only polyploidization (parameter ρ , the transition rate from *D* to *P*), but also diploidization (parameter δ , the transition rate from *P* to *D*).

Our second model assesses the signal of diversification due to ploidy differences while also parsing out the heterogeneity of diversification rates due a possible unobserved trait. BiSSE-like models can suffer from a large false discovery rate because they fail to account for diversification rate changes that do not directly depend on the trait of interest (Rabosky and Goldberg 2015; Beaulieu and O’Meara 2016). Diversification rate differences explained by something (trait) other than ploidy, are accommodated by adding a hidden state (HiSSE model; Beaulieu and O’Meara 2016). In this model, each of the observed diploid and polyploid states is subdivided by a binary hidden trait with states *A* and *B*. We call this the *D/P–A/B ploidy and hidden state* model. We estimated the posterior probability distributions of speciation rates ($\lambda_{D_A}, \lambda_{D_B}, \lambda_{P_A}, \lambda_{P_B}$), extinction rates ($\mu_{D_A}, \mu_{D_B}, \mu_{P_A}, \mu_{P_B}$), net diversification rates ($r_{D_A}, r_{D_B}, r_{P_A}, r_{P_B}$), and relative extinction rates ($v_{D_A}, v_{D_B}, v_{P_A}, v_{P_B}$). In this model polyploidization rate ρ and diploidization rate δ are also included, and changes between hidden states are symmetrical with rate α .

Models for breeding system and diversification

To assess the effects of breeding system in the diversification process, we first fit model in which the states are self-incompatible (I) or self-compatible (C). This is the same as the analysis of Goldberg et al. (2010), save for an updated phylogeny (Särkinen et al. 2013). We call this BiSSE model the *I/C breeding system* model. To parse out the effect of breeding system on diversification, while allowing for the possibility of heterogeneous diversification rates unrelated to breeding system, we subdivided each of those states into hidden states *A* and *B*. We call this HiSSE model the *I/C–A/B breeding system and hidden state* model.

For all breeding system models, we allow transitions from *I* to *C* (at rate q_{IC}) but not the reverse. Within Solanaceae, self-incompatibility is homologous in all species in which S-alleles were cloned, and controlled crosses performed. All species sampled to date, possess a non-self recognition, RNase-based, gametophytic self-incompatibility (shared even shared even with other euasterid families; Ramanauskas and

Igić 2017). Furthermore, species that are distantly related within this family carry closely-related alleles, with deep trans-specific polymorphism, at the S-locus, which controls the SI response (Ioerger et al. 1990; Igić et al. 2006). This represents very strong evidence that the SI mechanism, and our *I* state is ancestral to the Solanaceae, and did not arise independently within the family ($q_{CI} = 0$).

Models for ploidy, breeding system, and diversification

If ploidy and breeding system each influence lineage diversification individually, it is logical to examine their possible joint effects. We thus fit a multi-state model that includes both traits (MuSSE, FitzJohn 2012). The three states in this model are self-incompatible diploids (ID), self-compatible diploids (CD), and polyploids, which are always self-compatible (CP). As explained above, we did not include a state for self-incompatible polyploids because they are not observed in the data, and that trait combination state is mechanistically predicted not to occur. We call this the *ID/CD/CP ploidy and breeding system* model. The model has 10 parameters, six for diversification in each state (λ_{ID} , λ_{CD} , λ_{CP} for speciation, μ_{ID} , μ_{CD} , μ_{CP} for extinction) and four for transitions between states (ρ_I , ρ_C for polyploidization transitions from *ID* and *CD* to *CP*, respectively; δ for diploidization from *CP* to *CD*; q_{IC} for loss of self-incompatibility without polyploidization, from *ID* to *CD*). The total rate of loss of self-incompatibility, i.e., transitions out of *ID*, is $q_{IC} + \rho_I$. Diploidization from *CP* to *ID* is not allowed because it would represent a simultaneous regain of SI.

The ID/CD/CP model could potentially capture similar dynamics as earlier models, if the effects of the hidden state in D/P–A/B were effectively caused by breeding system (or its correlates), and the hidden state in I/C–A/B was effectively caused by ploidy. There is also the potential, however, for a hidden factor to be influencing diversification beyond both of our focal traits, and this could again mislead inferences. We therefore added a hidden trait layer on top of our three-state model (analogous to Caetano et al. 2018; Herrera-Alsina et al. 2018; Huang et al. 2018). We refer to this as the *ID/CD/CP–A/B* model. A fully parameterized version of this model would have 26 rate parameters (Herrera-Alsina et al. 2018). Because our goal was to look for diversification rate differences associated with ploidy and breeding system rather than the specific effects of the hidden states, we fitted a simplified version with 16 parameters. The reduction in parameter space is achieved by fixing the rates for transitions among hidden states to be equal with rate α , and fixing the transition rates between observed states to be independent of the hidden state (rates ρ_I , ρ_C , δ , q_{IC} as defined for the ID/CD/CP model). There are additionally twelve diversification rate parameters (λ_{ID_A} , λ_{ID_B} , λ_{CD_A} , λ_{CD_B} , λ_{CP_A} , λ_{CP_B} , μ_{ID_A} , μ_{ID_B} , μ_{CD_A} , μ_{CD_B} , μ_{CP_A} , μ_{CP_B}).

Diploidization as an exploratory hypothesis

For all four models that consider ploidy changes, we allowed diploidization. Previous modeling approaches (Mayrose et al. 2011) have argued against inferring diploidization rates when using ploidy data that comes from classifications based on chromosome number multiplicity or chromosome number change models like chromEvol (Mayrose et al. 2010). These types of classifications do not allow for a ploidy reversion. Where indicated, the classification of ploidy for the data used in our models was based on chromosome multiplicity at the genus level. However, the majority of the ploidy classifications were adopted from original studies with alternative sources of information (e.g., geographic distribution, genus ploidy distribution) where ploidy was defined by authors that found evidence for it. Since it is not clear whether diploidization can be detected under alternative ploidy classifications or even classifications based on chromosome number multiplicity at the genus level, we also fit the models without diploidization in order to test whether the conclusions about diversification are sensitive to including diploidization. As discussed by Servedio et al. (2014), the presence or absence of a hypothesis can have an exploratory goal. In our case the diploidization parameter (or its absence, $\delta = 0$) in our models is an opportunity to explore an assumption that might be important but that is not the single definitive process to understand the interactions among polyploidy, breeding system, and diversification.

Statistical inference under the models

Parameters for each of the 10 diversification models were performed using custom code in the RevBayes (Höhna et al. 2016) environment. Code for analyses and key results is available at <https://github.com/roszenil/solploidy>. We included a correction for incomplete sampling in all analyses, based on assuming that the Solanaceae family has approximately 3,000 species ($s = 595/3000$) as estimated by the Solanaceae Source project (PBI *Solanum* Project 2012). For all 10 models, we assumed that speciation and extinction parameters had log-normal prior distributions with means equal to the expected net diversification rate (number of taxa/ $[2 \times \text{root age}]$) and standard deviation 0.5. Priors for parameters defining trait changes were assumed to be gamma distributed with parameters $k = 0.5$ and $\theta = 1$. For each model, an MCMC chain was run for 96 hours in the high-performance computational cluster at the Minnesota Supercomputing Institute, which allowed for 5,000 generations of burn-in and a minimum of 200,000 generations of MCMC for each of the 6 models. For each model, convergence and mixing of the MCMC was tested using the R library coda and the software package Tracer (see supplementary information for convergence plots).

Model selection

We calculated the marginal likelihood for each of the 10 models in RevBayes (Höhna et al. 2016). Marginal
200 likelihoods were calculated using 50 stepping stone steps under the methodology of Xie et al. (2010). Each
stepping stone step was found by calculating 500 generations of burn-in followed by a total of 1,000 MCMC
steps (Table 1). The calculation of each marginal likelihood ran for 24 hours on a high-performance com-
putational cluster.

Using the marginal likelihood values, we calculated thirteen different Bayes factors. Six compared
205 the models of polyploidy against each other (D/P and D/P–A/B, each with or without diploidization), one
compared the breeding system models (I/C and I/C–A/B), and six compared the models with both traits
(ID/CD/CP and ID/CD/CP–A/B, each with or without diploidization) (Table 2). Other comparisons between
these models are not valid because the input data are different under the different state space codings (Fig. 1).
In essence, the D/P, I/C, and ID/CD/CP state spaces are not lumpable with respect to one another (Tarasov
210 2018).

Results

Polyploidy and Diversification Models

Similarly to the results obtained by Mayrose et al. (2011) and Mayrose et al. (2015), we found that in the D/P
polyploidy model the net diversification of diploids is larger than the the net diversification of polyploids
215 since the net diversification distributions do not overlap (Figure 2(A)). This result holds true whether or not
the diploidization parameter is present. However in the presence of the diploidization parameter the net
diversification rate of polyploids is nonnegative with probability 1 (Figure 2(A)), whereas in the absence
of diploidization the net diversification rate of polyploids can be negative with a probability (HERE verify
the quantile) (FIGURE 3(A)). In terms of the relative extinction, when the diploidization parameter is
220 present both polyploids and diploids have posterior distributions that overlap, but that pattern changes in
the absence of the diploidization parameter leading to a significant difference between relative extinction
where polyploids have a significant higher relative extinction rate (see Supplementary Information).

For the D/P- A/B model with diploididization the diploid and polyploid net diversification rates
225 are overlapping for both state A and B of the hidden trait (Figure 2(B)). In this model, the differences in
net diversification are due to the presence of a hidden trait and not to the differences in ploidy. When
diploidization parameter is absent the hidden state is still driving the differences in diversification rates
(Figure 3(B)).

Breeding System and Diversification models

230 In the I/C breeding system model we found that the net diversification rate for self-incompatible state is larger than the net diversification rate for self-compatible state (Figure 2(C)). The net diversification rate for self-compatible has a probability distribution centered at zero.

235 When a hidden state is added in the I/C-A/B model, we found that under the hidden state A the self-compatible and self-incompatible net diversification rates are different. Under the hidden state B, those two rates overlap with a probability (HERE CALCULATE THAT) meaning that they are different with probability (CALCULATE) (Figure 2(D)). These results agree with previous results found by Goldberg and Igić (2012). However, Goldberg and Igić (2012) used a ClaSSE approach since they were interested in anagenetic and cladogenetic changes for self-incompatibility using a smaller subset of the data presented in
240 the current work.

Polyploidy and Breeding Sytem models

In the ID/P/CD model we found that self-incompatible and diploid state has a significantly larger net diversification rate compare to both self-compatible diploid and polyploid rates. Meanwhile, both self-compatible diploid and polyploid posterior distributions of net diversification rates completely overlap (Figure 2(E)).

245 When hidden state was added in the ID/P/CD-A/B model, we observed significant differences between self-compatible and self-incompatible diploids for both A and B values of the hidden state. Self-incompatible state had a larger net diversification rate than self compatible for both A and B states. However, the posterior distribution for the net diversification rate of polyploids overlaps with both the self-compatible and self-incompatible posterior distributions for each value of the hidden state(Figure 2F) meaning that polyploidy state is not significantly different from diploid in net diversification terms. The resulting effect of
250 adding the hidden state values is significant

Diploidization as an exploratory hypothesis

In the D/P model the diploidization rate δ and polyploidization rate ρ are different from zero with probability 1. Diploidization rate is more uncertain than polyploidization. For the D/P no δ model, the
255 polyploidization rate is still different from zero but has a wider 95% credible interval (see Supplementary Information). In the D/P-A/B model the diploidization rate remains positive but there rate of polyploidization becomes really uncertain. Whereas, in the absence of diploidzation (D/P no δ A/B) the rate of polyploidy has a small credible interval

For the model ID/P/CD containing both polyploidy and breeding system traits, we found that the diploidization rate is really uncertain with a MAP that is (CALCULATE VALUE HERE- close to zero). The polyploidization rate from self-incompatible diploid ρ_I is slightly faster than the polyploidization rate from self-compatible diploid ρ_C and that pattern remains the same for the ID/P no δ /CD model(see supplementary information).

Model selection

In Table 1 we list the marginal likelihood in log scale for each of the models tested. In the table we show what are the different components included and excluded for each model as a summary of the diagrams from Fig. 2. From the marginal likelihoods in log scale, the Bayes factors in log-scale were calculated as shown in table Table 2. After testing every single pair of polyploidy modes (1-4) we found overwhelming evidence that the best polyploidy model is always the D/P-A/B, that is the model with hidden state and diploidization.

For the two models following the evolution of breeding system, the I/C-A/B is the best choice between models 3 and 4.

The models that follow the diversification linked to both polyploidy and breeding system are the last 4 (models 5-8). When comparing using Bayes factors every two models we found that the IC/P/CD-A/B is always preferred over the rest, meaning that the model that has a hidden state and diploidization is chosen over the ones that lack either of both of those options.

Therefore, the models that were chosen were always the ones containing a hidden trait, and in the case of polyploidy models, the ones containing a diploidization parameter δ are preferable.

Discussion

Acknowledgements

NSF DEB-1655478. The Minnesota Supercomputing Institute (MSI) at the University of Minnesota provided computing resources for this project.

Literature Cited

- Barrett, S. C., 1988. The evolution, maintenance, and loss of self-incompatibility systems, vol. Plant reproductive ecology: patterns and strategies, Pp. 98–124. Oxford University Press Oxford.
- , 2008. Major evolutionary transitions in flowering plant reproduction: an overview.
- , 2013. The evolution of plant reproductive systems: how often are transitions irreversible? *Proceedings of the Royal Society B: Biological Sciences* 280:20130913.
- Barringer, B. C., 2007. Polyploidy and self-fertilization in flowering plants. *American Journal of Botany* 94:1527–1533.
- Beaulieu, J. M. and B. C. O’Meara, 2016. Detecting hidden diversification shifts in models of trait-dependent speciation and extinction. *Syst Biol* 65:583–601.
- Bennett, M. D. and I. J. Leitch, 2005. Plant DNA C-values database.
- Caetano, D. S., B. C. O’Meara, and J. M. Beaulieu, 2018. Hidden state models improve state-dependent diversification approaches, including biogeographical models. *Evolution* 72:2308–2324.
- Camadro, E. and S. J. Peloquin, 1981. Cross-incompatibility between two sympatric polyploid *Solanum* species. *Theoretical and Applied Genetics* 60:65–70.
- Charlesworth, D., 1985. Distribution of dioecy and self-incompatibility in angiosperms. *Evolution: essays in honour of John Maynard Smith* Pp. 237–268.
- Entani, T., S. Takayama, M. Iwano, H. Shiba, F.-S. Che, and A. Isogai, 1999. Relationship between polyploidy and pollen self-incompatibility phenotype in *Petunia hybrida* Vilm. *Bioscience, Biotechnology, and Agrochemistry* 63:1882–1888.
- FitzJohn, R. G., 2012. Diversitree : comparative phylogenetic analyses of diversification in r. *Methods Ecol Evol* 3:1084–1092.
- FitzJohn, R. G., W. P. Maddison, and S. P. Otto, 2009. Estimating trait-dependent speciation and extinction rates from incompletely resolved phylogenies. *Systematic Biology* 58:595–611.
- Goldberg, E. E. and B. Igić, 2012. Tempo and mode in plant breeding system evolution. *Evolution* 66:3701–3709.
- Goldberg, E. E., J. R. Kohn, R. Lande, K. A. Robertson, S. A. Smith, and B. Igić, 2010. Species selection maintains self-incompatibility. *Science* 330:493–495.
- Herrera-Alsina, L., P. van Els, and R. S. Etienne, 2018. Detecting the dependence of diversification on multiple traits from phylogenetic trees and trait data. *Systematic biology* .
- Höhna, S., M. J. Landis, T. A. Heath, B. Boussau, N. Lartillot, B. R. Moore, J. P. Huelsenbeck, and F. Ronquist, 2016. Revbayes: Bayesian phylogenetic inference using graphical models and an interactive model-specification language. *Systematic Biology* 65:726–736.
- Huang, D., E. E. Goldberg, L. Chou, and K. Roy, 2018. The origin and evolution of coral species richness in a marine biodiversity hotspot. *Evolution* 72:288–302.
- Husband, B. C., B. Ozimec, S. L. Martin, and L. Pollock, 2008. Mating consequences of polyploid evolution in flowering plants: Current trends and insights from synthetic polyploids. *International Journal of Plant Sciences* 169:195–206.
- Igić, B., L. Bohs, and J. R. Kohn, 2006. Ancient polymorphism reveals unidirectional breeding system shifts. *Proc Natl Acad Sci USA* 103:1359–1363.
- Ioerger, T. R., A. G. Clark, and T. H. Kao, 1990. Polymorphism at the self-incompatibility locus in Solanaceae predates speciation. *Proceedings of the National Academy of Sciences USA* 87:9732–9735.
- Kubo, K.-i., T. Entani, A. Takara, N. Wang, A. M. Fields, Z. Hua, M. Toyoda, S.-i. Kawashima, T. Ando, A. Isogai, et al., 2010. Collaborative non-self recognition system in s-rnase-based self-incompatibility. *Science* 330:796–799.
- Lewis, D., 1947. Competition and dominance of incompatibility alleles in diploid pollen. *Heredity* 1:85–

108.

Lynch, M. and J. S. Conery, 2000. The evolutionary fate and consequence of duplicate genes. *Science* 290:1151–1155.

Maddison, W. P. and R. G. FitzJohn, 2014. The unsolved challenge to phylogenetic correlation tests for categorical characters. *Systematic biology* 64:127–136.

Maddison, W. P., P. E. Midford, and S. P. Otto, 2007. Estimating a binary character's effect on speciation and extinction. *Syst Biol* 56:701–710.

Mayrose, I., M. S. Barker, and S. P. Otto, 2010. Probabilistic models of chromosome number evolution and the inference of polyploidy. *Systematic Biology* 59:132–144.

Mayrose, I., S. H. Zhan, C. J. Rothfels, N. Arrigo, M. S. Barker, L. H. Rieseberg, and S. P. Otto, 2015. Methods for studying polyploid diversification and the dead end hypothesis: a reply to soltis et al. (2014). *New Phytol* 206:27–35.

Mayrose, I., S. H. Zhan, C. J. Rothfels, K. Magnuson-Ford, M. S. Barker, L. H. Rieseberg, and S. P. Otto, 2011. Recently formed polyploid plants diversify at lower rates. *Science* 333:1257.

Olmstead, R. G. and L. Bohs, 2007. A summary of molecular systematic research in Solanaceae: 1982–2006. *Acta Horticulturae* Pp. 255–268.

PBI *Solanum* Project, 2012. Solanaceae Source: a global taxonomic resource for the nightshade family.

Rabosky, D. L. and E. E. Goldberg, 2015. Model inadequacy and mistaken inferences of trait-dependent speciation. *Systematic Biology* 64:340–355.

Raduski, A. R., E. B. Haney, and B. Igić, 2012. The expression of self-incompatibility in angiosperms is bimodal. *Evolution* 66:1275–1283.

Ramanauskas, K. and B. Igić, 2017. The evolutionary history of plant t2/s-type ribonucleases. *PeerJ* 5:e3790.

Ramsey, J. and D. W. Schemske, 1998. Pathways, mechanisms, and rates of polyploid formation in flowering plants. *Annual Review of Ecology and Systematics* 29:467–501.

Rice, A., L. Glick, S. Abadi, M. Einhorn, N. M. Kopelman, A. Salman-Minkov, J. Mayzel, O. Chay, and I. Mayrose, 2015. The chromosome counts database (CCDB) - a community resource of plant chromosome numbers. *New Phytol* 206:19–26.

Rivero, R., E. B. Sessa, and R. Zenil-Ferguson, 2019. Eyechrom and cddb curator: Visualizing chromosome count data from plants. *Applications in Plant Sciences* P. e01207.

Robertson, K., E. E. Goldberg, and B. Igić, 2011. Comparative evidence for the correlated evolution of polyploidy and self-compatibility in solanaceae. *Evolution* 65:139–155.

Särkinen, T., L. Bohs, R. G. Olmstead, and S. Knapp, 2013. A phylogenetic framework for evolutionary study of the nightshades (Solanaceae): a dated 1000-tip tree. *BMC Evol Biol* 13:214.

Servedio, M. R., Y. Brandvain, S. Dhole, C. L. Fitzpatrick, E. E. Goldberg, C. A. Stern, J. Van Cleve, and D. J. Yeh, 2014. Not just a theory?the utility of mathematical models in evolutionary biology. *PLoS biology* 12:e1002017.

Stebbins, G. L., 1938. Cytological characteristics associated with the different growth habits in the dicotyledons. *American Journal of Botany* 25:189–198.

———, 1950. *Variation and Evolution in Plants*. Columbia University Press, New York.

———, 1974. *Flowering plants: evolution above the species level*. Belknap Press of Harvard University Press, Cambridge, Mass.

Stone, J. L., 2002. Molecular mechanisms underlying the breakdown of gametophytic self-incompatibility. *The Quarterly Review of Biology* 77:17–30.

Stout, A. B. and C. Chandler, 1942. Hereditary transmission of induced tetraploidy and compatibility in fertilization. *Science* 96:257–258.

Tarasov, S., 2018. Integration of anatomy ontologies and evo-devo using structured markov models suggests a new framework for modeling discrete phenotypic traits. *BioRxiv* P. 188672.

380 Tsukamoto, T., T. Ando, H. Watanabe, E. Marchesi, and T.-h. Kao, 2005. Duplication of the s-locus f-box gene is associated with breakdown of pollen function in an s-haplotype identified in a natural population of self-incompatible *petunia axillaris*. *Plant Molecular Biology* 57:141–153.

Vision, T. J., D. G. Brown, and S. D. Tanksley, 2000. The origins of genomic duplications in *Arabidopsis*. *Science* 290:2114–2117.

385 de Vos, J. M., C. E. Hughes, G. M. Schneeweiss, B. R. Moore, and E. Conti, 2014. Heterostyly accelerates diversification via reduced extinction in primroses. *Proceedings of the Royal Society B: Biological Sciences* 281:20140075.

Xie, W., P. O. Lewis, Y. Fan, L. Kuo, and M.-H. Chen, 2010. Improving marginal likelihood estimation for bayesian phylogenetic model selection. *Systematic biology* 60:150–160.

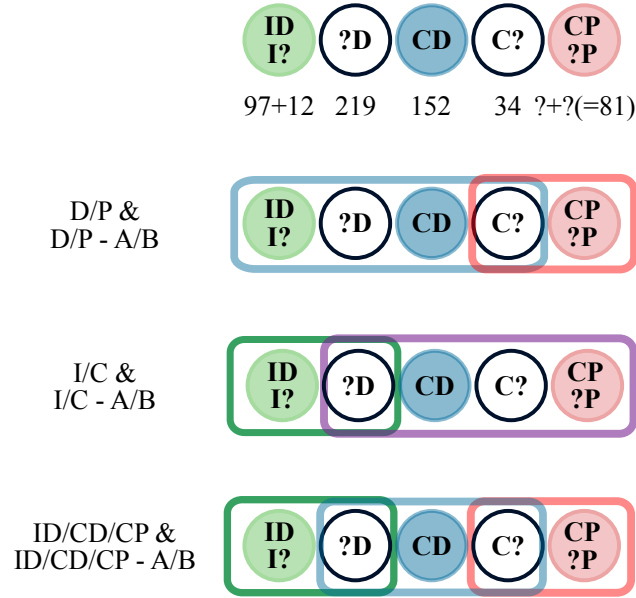


Figure 1: Character states used for each of the models. Each species retained on the tree belonged to one of five possible categories, depending on whether ploidy and/or breeding system were known. The number of species in each is shown under the corresponding circles in the top row. These categories were then grouped in a manner appropriate to the states of each model. For example, there are 34 species that are self-compatible and of unknown ploidy; these are coded as either *D* or *P* in the D/P models (uncertain, or consistent with either state), as *C* in the I/C models, and as either *CD* or *CP* in the ID/CD/CP models. In all cases, species were coded as either *A* or *B* in the hidden state models.

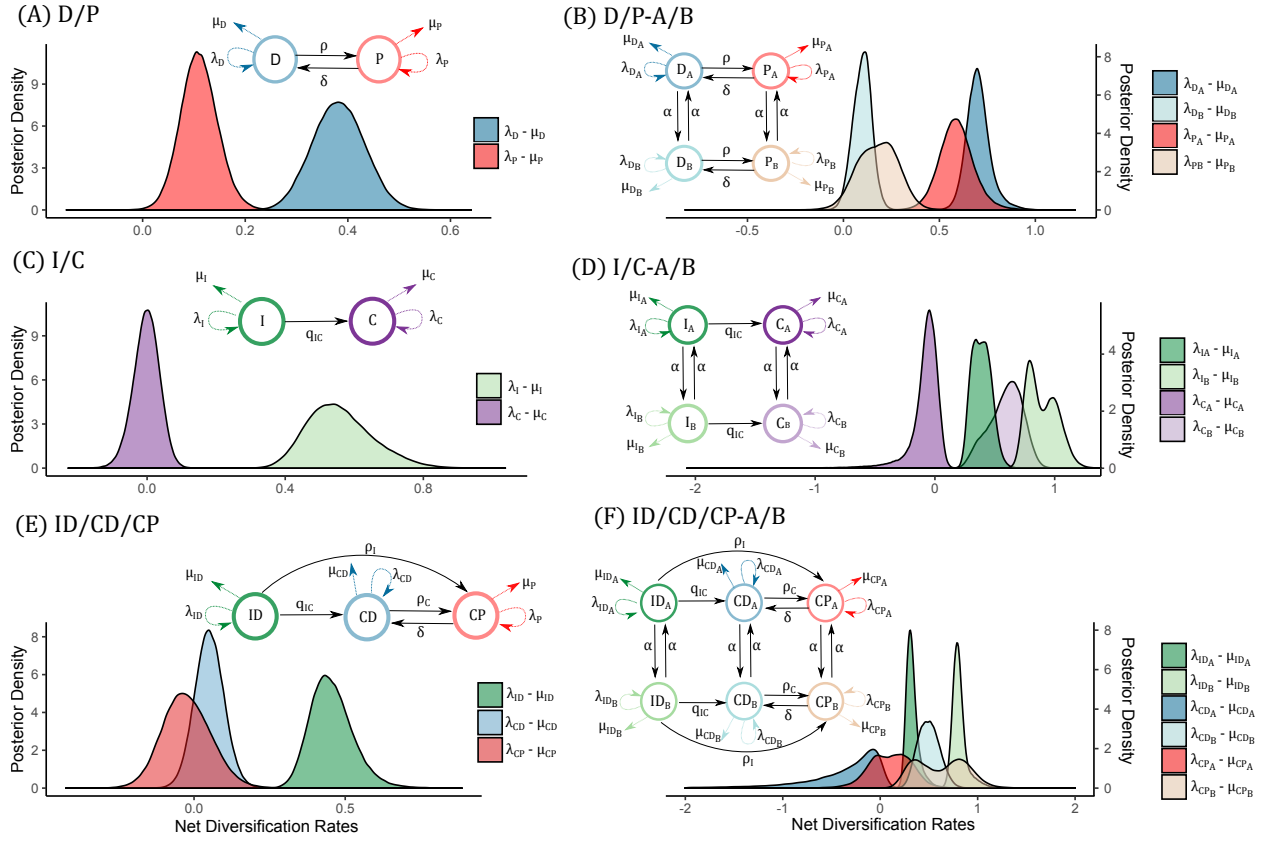


Figure 2: Net diversification rates for all models that include diploidization.

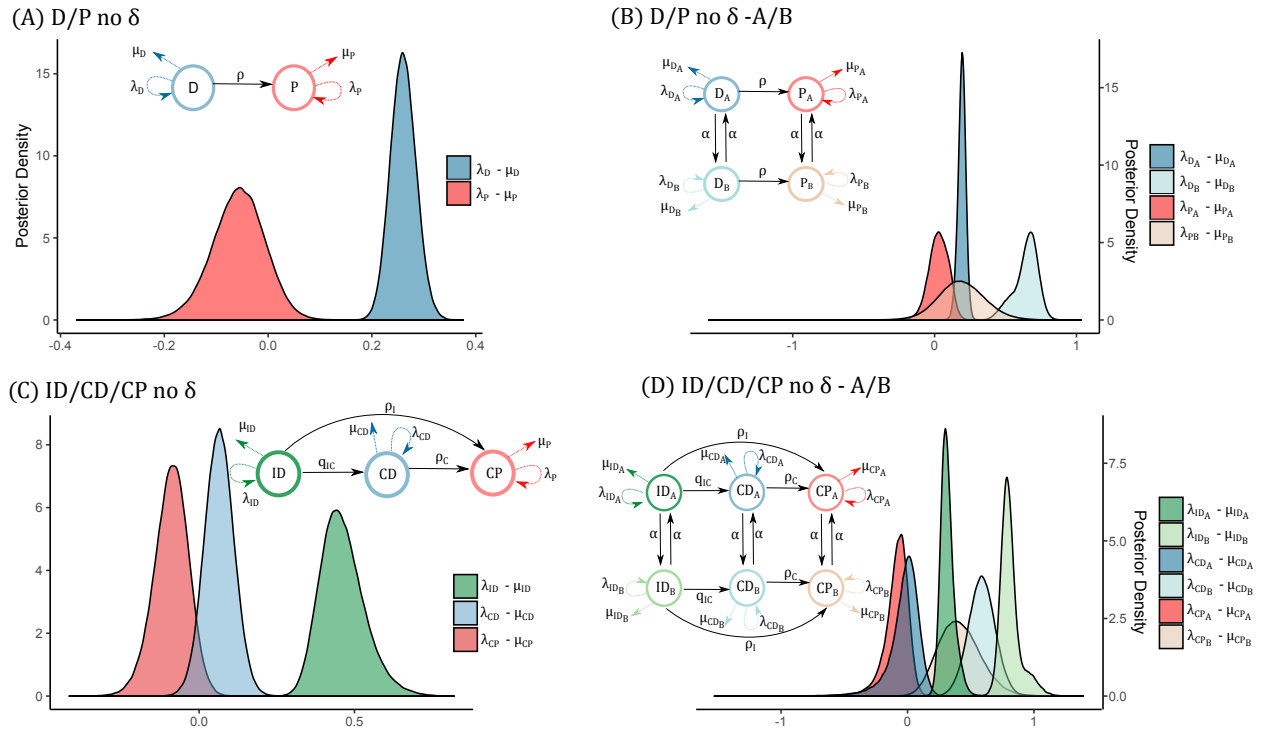


Figure 3: Net diversification rates for all models that do not include diploidization.

Model	Model Type	Ploidy	Diploidization	Breeding System	Hidden State	Parameters	Marginal Log- Likelihood
1. D/P	BiSSE	Yes	Yes	No	No	6	-1182.93
2. D/P no δ	BiSSE	Yes	No	No	No	5	-1193.66
3. D/P- A/B	HiSSE	Yes	Yes	No	Yes	11	-1145.69
4. D/P no δ -A/B	HiSSE	Yes	No	No	Yes	10	-1150.99
5. I/C	BiSSE	No	No	Yes	No	5	-1194.80
6. I/C-A/B	HiSSE	No	No	Yes	Yes	10	-1155.37
7. ID/P/CD	MuSSE	Yes	Yes	Yes	No	10	-1344.50
8. ID/P/CD no δ	MuSSE	Yes	No	Yes	No	9	-1345.87
9. ID/P/CD-A/B	MuHiSSE	Yes	Yes	Yes	Yes	16	-1300.35
10.ID/P/CD no δ -A/B	MuHiSSE	Yes	No	Yes	Yes	15	-1303.55

Table 1: Marginal likelihoods for the ten models examined. States encoded with letter D: diploid, P: polyploid, C: self-compatible, I: self-incompatible, A: first state of hidden trait, B: second state of hidden trait, δ : re-diploidization.

Ploidy Models					Breeding System Models		Ploidy and Breeding System Models					
	1	2	3	4		5	6		7	8	9	10
1. D/P	·	10.72	-37.24	-31.94	5. I/C	·	-39.43	7. ID/P/CD	·	1.36	-44.15	-40.95
2. D/P no δ	·	·	-47.97	-42.66	6. I/C-A/B	·	·	8. ID/P/CD no δ	·	·	-45.51	-42.31
3. D/P- A/B	·	·	·	5.30				9. ID/P/CD-A/B	·	·	·	3.2
4. D/P no δ -A/B	·	·	·	·				10. ID/P/CD no δ -A/B	·	·	·	·

Table 2: Bayes factors in log scale. We compare every possible pair. Number models as indicated in Table 1.

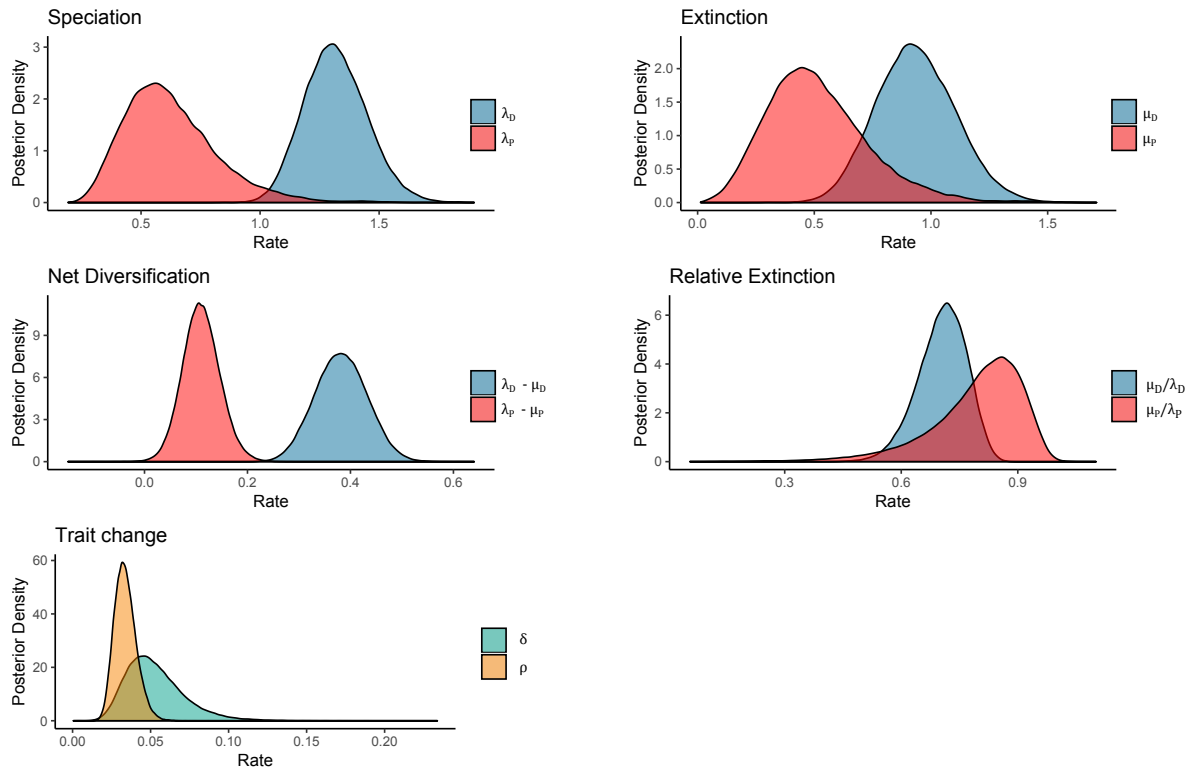


Figure S1: Posterior distribution for each of the parameters in the D/P polyploidy model

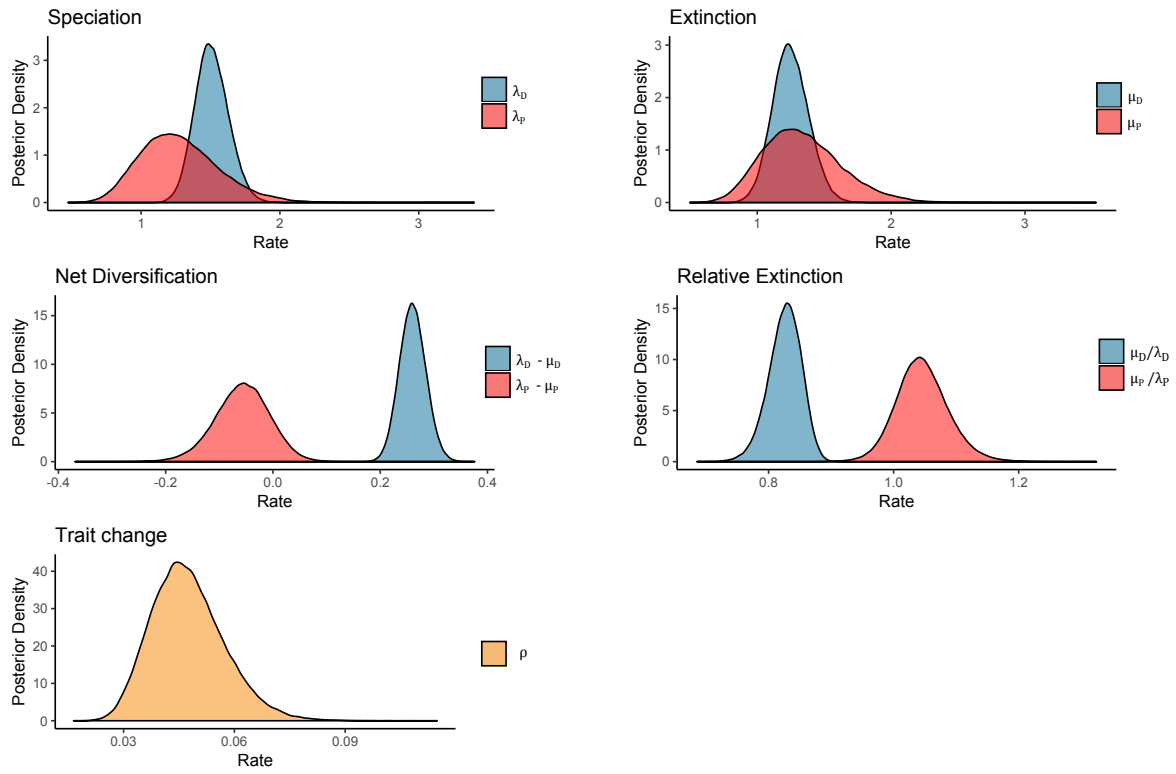


Figure S2: Posterior distribution for each of the parameters in the D/P no δ polyploidy model

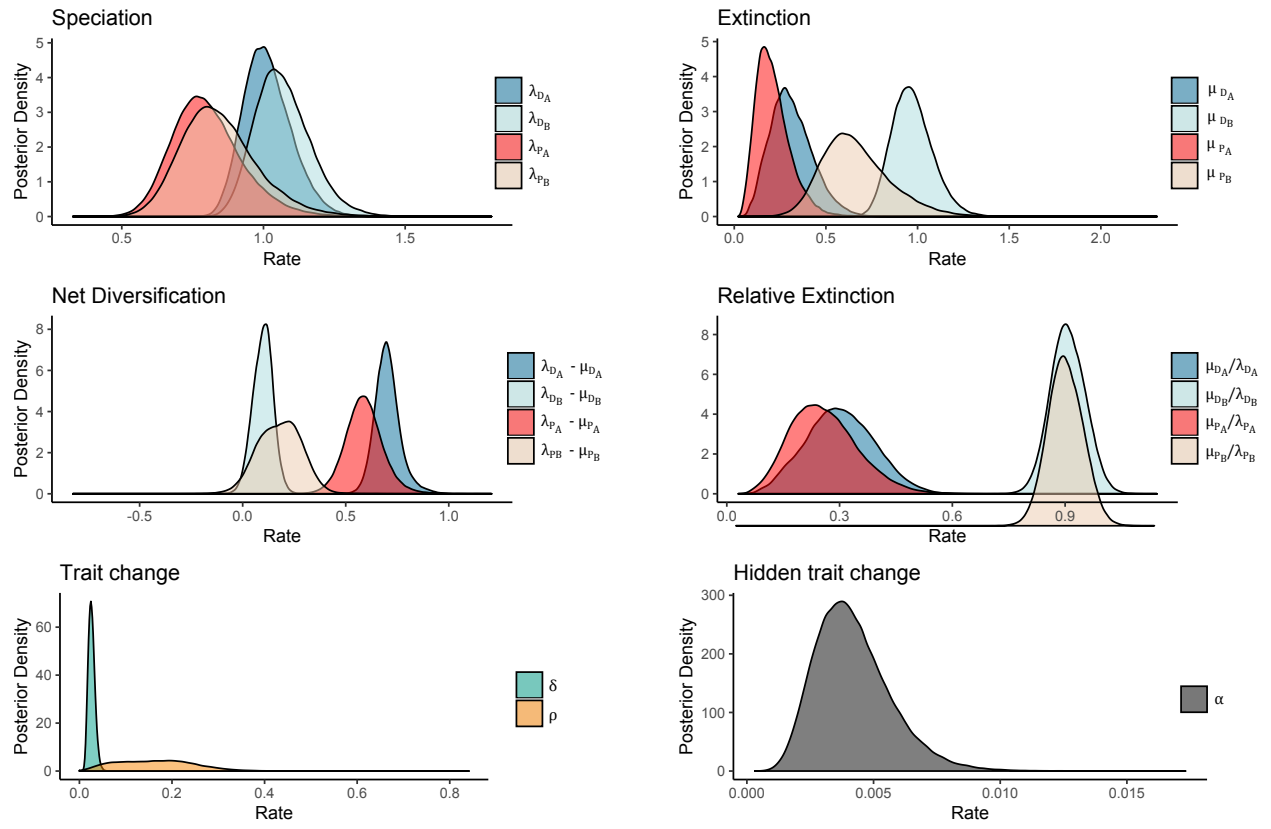


Figure S3: Posterior distribution for each of the parameters in the D/P-A/B polyploidy model

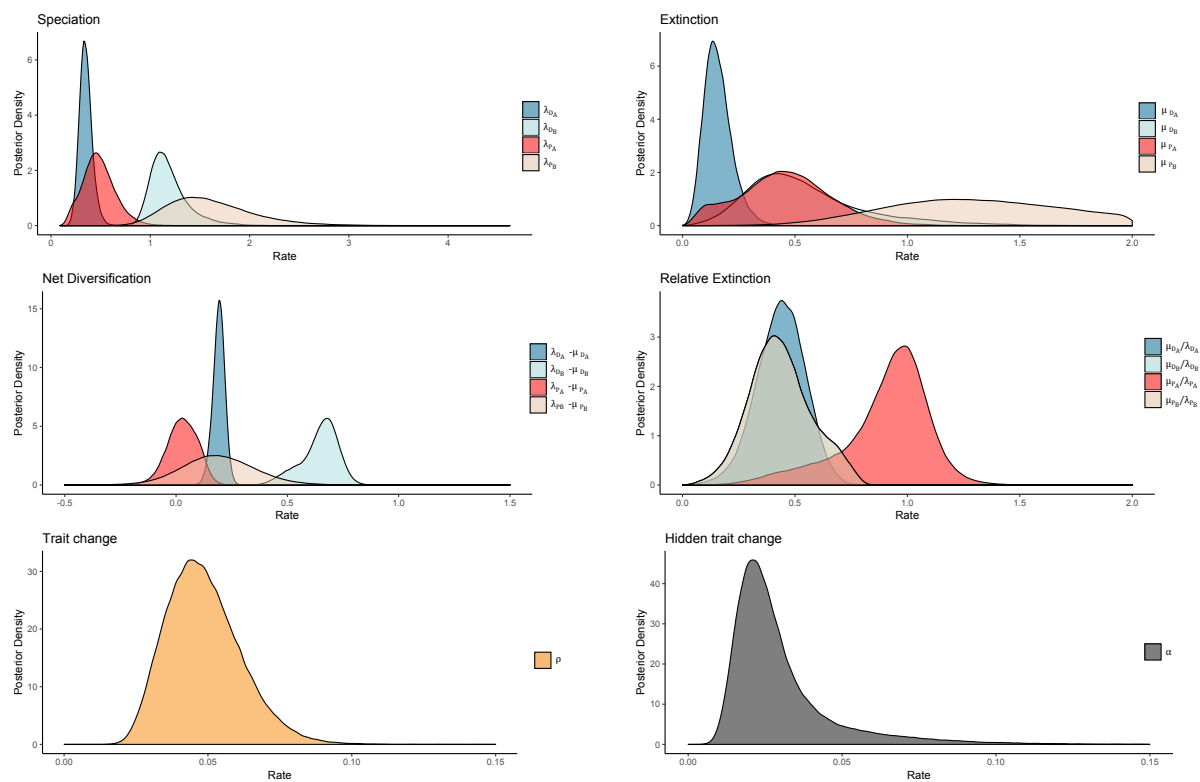


Figure S4: Posterior distribution for each of the parameters in the D/P no δ -A/B polyploidy model

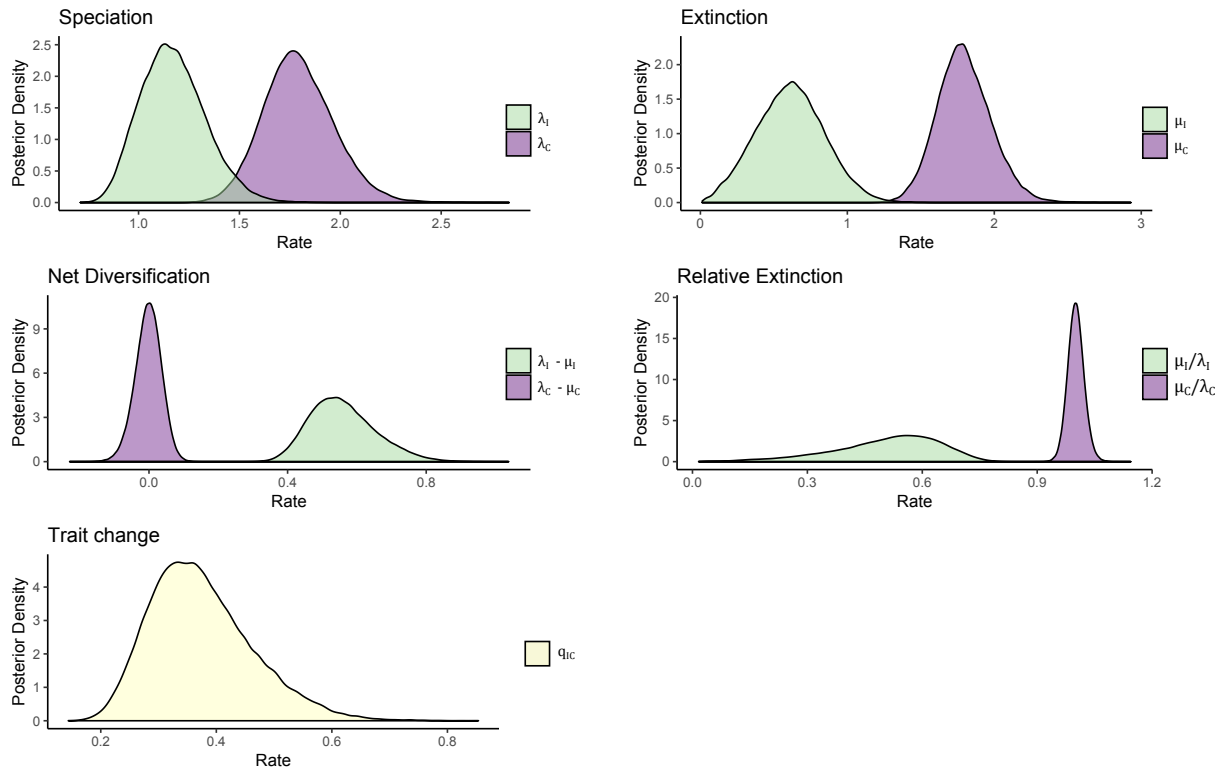


Figure S5: Posterior distribution for each of the parameters in the I/C breeding system model

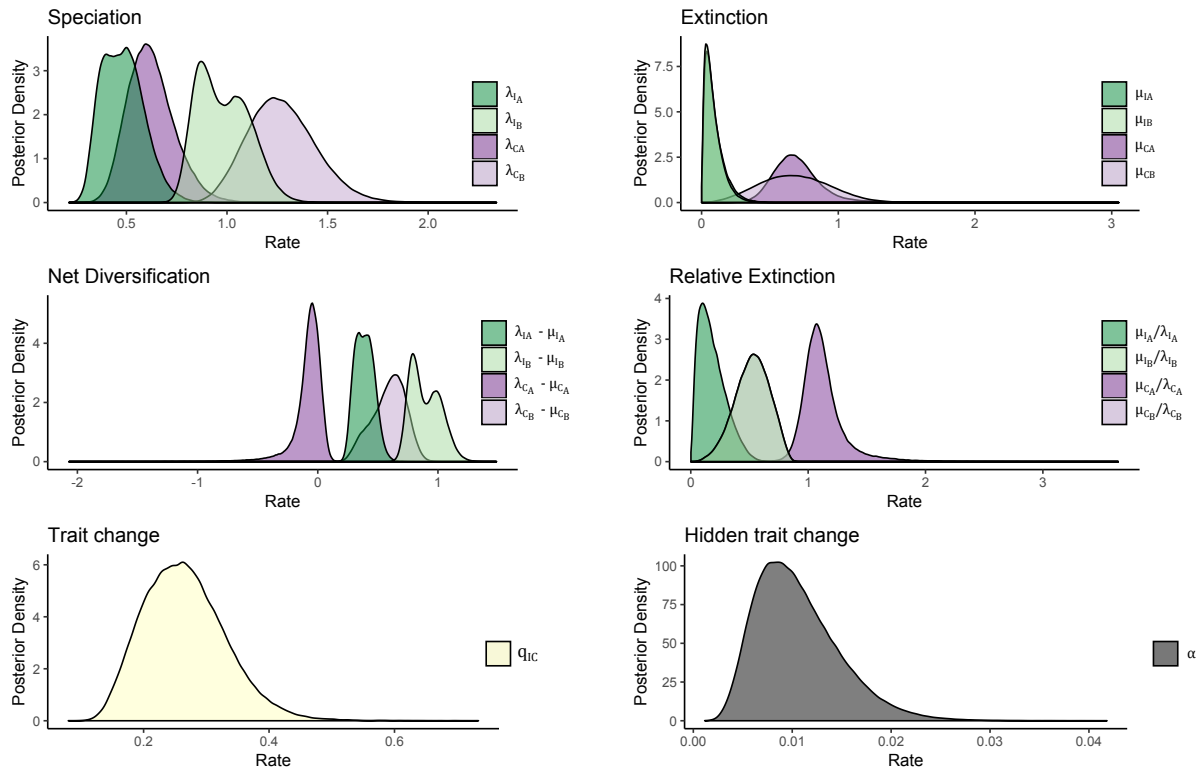


Figure S6: Posterior distribution for each of the parameters in the I/C-A/B breeding system model

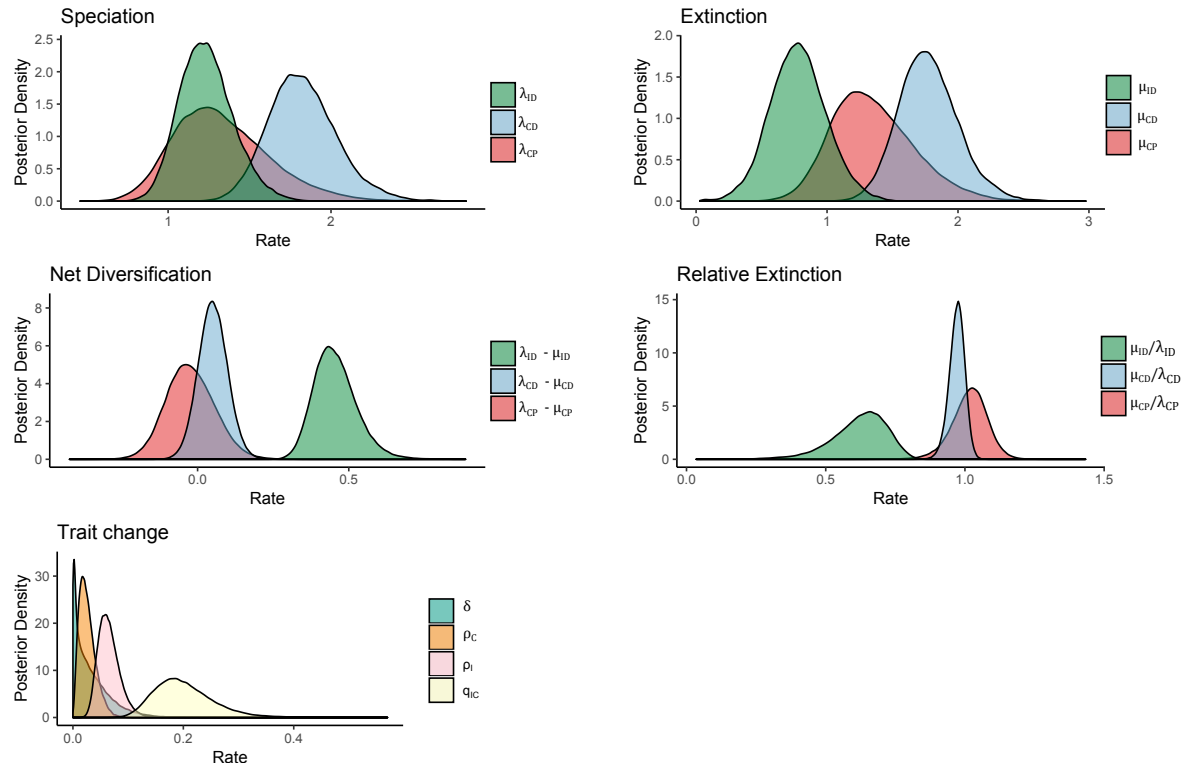


Figure S7: Posterior distribution for each of the parameters in the ID/CD/CP polyploidy and breeding system model

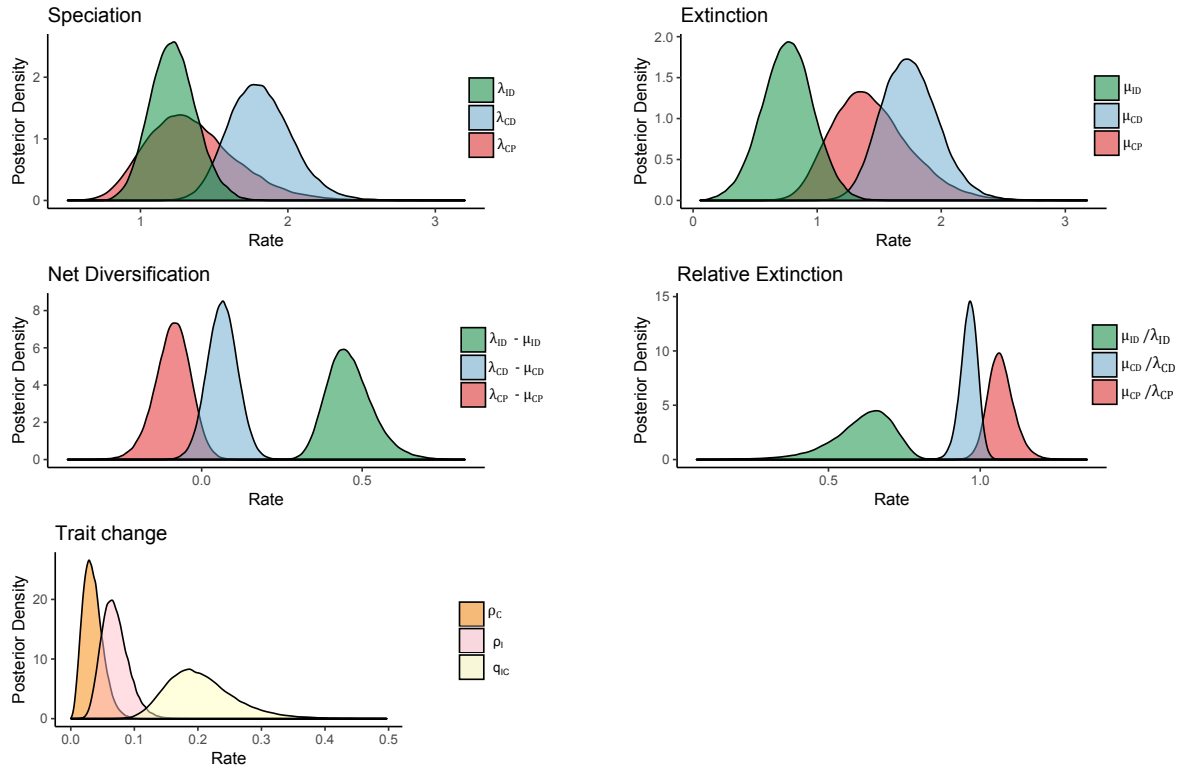


Figure S8: Posterior distribution for each of the parameters in the ID/CD/CP no δ polyploidy and breeding system model

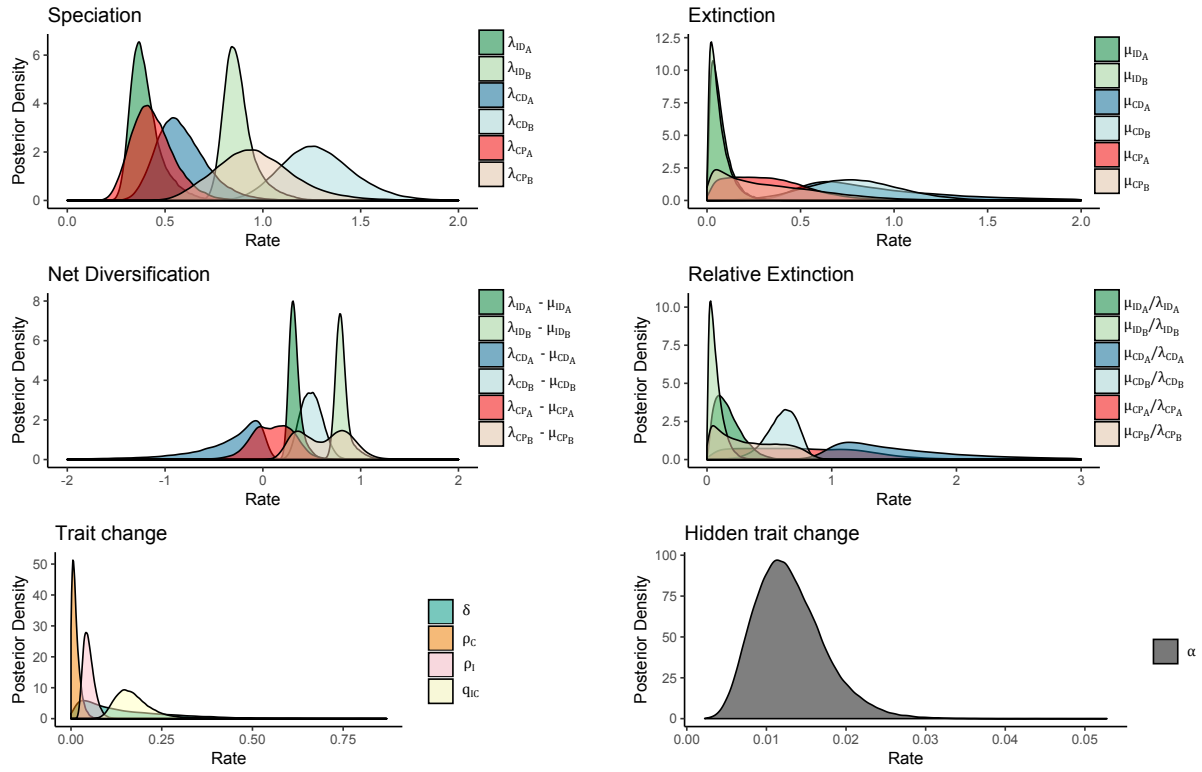


Figure S9: Posterior distribution for each of the parameters in the ID/CD/CP-A/B polyploidy and breeding system model

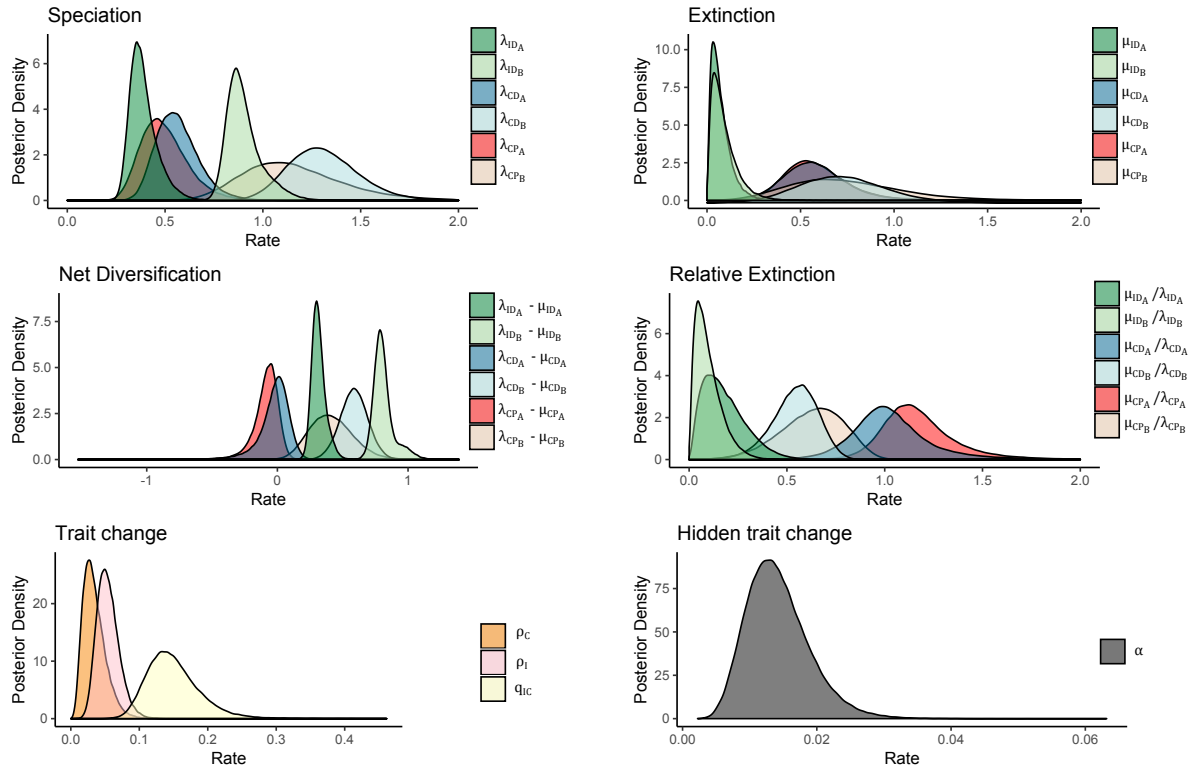


Figure S10: Posterior distribution for each of the parameters in the ID/CD/CP no δ - A/B polyploidy and breeding system model

	D/P	D/P+A/B	I/C	I/C+A/B	ID/CD/CP	ID/CD/CP+A/B
r_D			—	—	—	—
r_P			—	—	—	—
r_I	—	—			—	—
r_C	—	—			—	—
r_{ID}	—	—	—	—		
r_{CD}	—	—	—	—		
r_{CP}	—	—	—	—		
ρ			—	—	—	—
ρ_I	—	—	—	—		
ρ_C	—	—	—	—		
δ						
q_{IC}	—	—				
	D/P	D/P+A/B	I/C	I/C+A/B	ID/CD/CP	ID/CD/CP+A/B
r_D			—	—	—	—
r_P			—	—	—	—
r_I	—	—			—	—
r_C	—	—			—	—
r_{ID}	—	—	—	—		
r_{CD}	—	—	—	—		
r_{CP}	—	—	—	—		
ρ			—	—	—	—
ρ_I	—	—	—	—		
ρ_C	—	—	—	—		
q_{IC}	—	—				

Table S1: median rate estimates for all models (see supp figs for more details and uncertainties); when there are two numbers in one cell, they're for the A and B hidden states; — means that parameter was not present in the model; upper section is for models with δ and lower section is for models without